Chem Soc Rev

Photoinduced charge and energy transfer in molecular wires

SCHOLARONE™
Manuscripts

Photoinduced charge and energy transfer in molecular wires

Mélina Gilbert and Bo Albinsson[¤]

Department of Chemical and Biological Engineering / Physical Chemistry

Chalmers University of Technology, 412 96 Göteborg, Sweden

Email: balb@chalmers.se

Key learning points

- Photoinduced electron and energy transfer reactions
- Superexchange theory; coherent tunneling vs. incoherent hopping
- Molecular bridges (wires) and distance dependence of electron and energy transfer reactions
- Conformational dependence of electron and energy transfer processes in D-B-A systems
- Influence of the bridge topology on electron and energy transfer in porphyrin-based molecular wires

Abstract

Exploring charge and energy transport in donor-bridge-acceptor systems is an important research field which is essential for the fundamental knowledge necessary to develop future applications. These studies help creating valuable knowledge to respond to today's challenges to develop functionalized molecular systems for artificial photosynthesis, photovoltaics or molecular scale electronics. This tutorial review focuses on photo-induced charge/energy transfer in covalently linked donor-bridge-acceptor (D-B-A) systems. Of the utmost importance in such systems is to understand how to control signal transmission, i.e. how fast electrons or excitation energy could be transferred between the donor and acceptor and the role played by the bridge (the "molecular wire"). After a brief description of the electron and energy transfer theory, we aim to give a simple yet accurate picture of the complex role played by the bridge to sustain donor-acceptor electronic communication. Special emphasis is put on understanding bridge energetics and conformational dynamics effects on the distance dependence of the donor-acceptor electronic coupling and transfer rates. Several examples of donor-bridge-acceptor systems from the literature are described as a support to the discussion. Finally, porphyrin-based molecular wires are introduced, and the relationship between their electronic structure and photophysical properties are outlined. In strongly conjugated porphyrin systems, limitations of the

existing electron transfer theory to interpret the distance dependence of the transfer rates are also discussed.
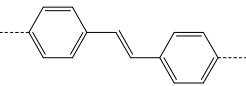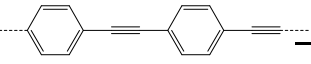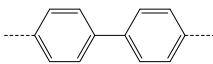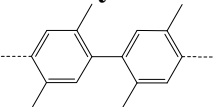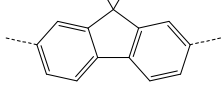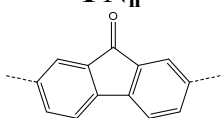
1. Introduction

Electron (ET) and Excitation Energy Transfer (EET) are key steps of many chemical and physical processes occurring in disciplines ranging from biology, chemistry, and physics to materials science. For instance, both processes constitute the *heart* of the natural photosynthesis.[1] In any natural photosynthetic system, light conversion into chemical energy requires a series of step-wise electron transfer processes to create a long lived charge separated state with sufficient energy for water oxidation and carbon dioxide reduction. Over the last two decades, mimicking these elementary steps in designed systems have attracted much interest, motivated by the technological potential of such systems in applications ranging from artificial photosynthesis to molecular electronics.[2] However, going from simple mimics to actual functioning devices is not simple and requires a thorough understanding of all parameters controlling ET and EET processes, especially the kinetics. In this context, considerable theoretical and experimental efforts have been devoted on identifying the factors that govern charge and hole transfer in molecular systems. Valuable knowledge has been acquired by experimentally studying ET and EET processes in donor-bridge-acceptor (D-B-A) mimics of the more complicated natural photosynthetic system. In such D-B-A systems, a donor (D) and an acceptor (A) are covalently linked using a molecular bridge (B). As bridge component, various structural motifs have been used. In this tutorial review, π-conjugated bridges consisting of covalently connected identical repetitive molecular motifs are considered. A list of such bridge structures, sometimes referred to as molecular wires, reported in the literature are summarized in Table 1 and these examples will form the spine of this discussion. The assets of π-conjugated bridges reside in their seeming rigidity, rod-like structure and more importantly their high degree of electron delocalization. The latter allows for substantial electronic communication between the individual bridge units and make them promising candidates for mediating charge/energy over long distances.

In D-B-A systems, ET and EET reactions are traditionally triggered using light excitation by selectively exciting either the donor or the acceptor. In the case of ET, these reactions are called photo-induced electron transfer (PET). However there exist other methods to investigate electron transfer in molecular systems. For instance, electron transfer through molecules can also be explored by placing single molecules between two metallic electrodes and measuring conductance. Such single molecule experiments are becoming increasingly popular as they approach more practical applications by using the molecule as an electrical interconnect between two devices.[3]

In this tutorial review, focus has been put on photo-induced electron and energy transfer in D-B-A systems, more particularly on the dependence of the transfer rates on distance, energetics and environment. For long range ET reactions through molecular structures governed by quantum mechanical tunneling, the so-called superexchange theory developed by McConnell already in 1961 is

often used.[4] The first part of the tutorial provides the reader with a brief description of the electron and energy transfer theory, which are intimately related. In the long range electron transfer field, distance dependence studies constitute a systematic experiment to probe the ability of a bridge to sustain charge transport. The ability of a bridge structure to mediate electronic coupling for ET have often been summarized in a single exponential decay constant, namely the attenuation factor β. However, several studies have shown that the use of the β-value as a simple descriptor of "conduction" is rather limited as this is not a bridge specific parameter, but instead a donor-bridge-acceptor ensemble parameter.[5] In this context, special emphasis of this tutorial is put on understanding the role of the bridge in charge/energy transfer processes in D-B-A systems. Several studies in carefully designed D-B-A systems have demonstrated that charge/energy transfer processes (i.e. kinetics and nature of the charge transport) in D-B-A are essentially governed by the bridge energetics[6] and conformational dynamics[7]. Implications of these studies for obtaining wire-like behavior of the molecular bridge (i.e. low β) are also discussed. To illustrate our discussion, selected examples from Table 1 are described in more details. Finally, the last part of the tutorial is dedicated to porphyrin-based molecular wires as interesting model systems for both long-range energy and electron transfer. Once more it is the bridge structure (i.e. the nature of the bridge linker and the linkage topology) that dictates the excitonic and/or electronic inter-porphyrin coupling in these conjugated porphyrin oligomers.[8] In particular, this was utilized to prepare molecular systems ideal for either energy or electron transfer.[9] Limitations of the McConnell model to describe electron transfer in strongly conjugated porphyrin systems are also discussed.

Table 1. Selected repeating bridge structures used to form D-B-A systems, along with the donor/acceptor couples. Estimations of tunneling barriers for charge separation and recombination and corresponding β-values are also given.

Bridge	D	A	n	ΔE_{CS} / eV	β_{CS} /Å⁻¹	ΔE_{CR} / eV	β_{CR} /Å⁻¹	Group/ref.
OPV	TET[a]	PI[b]	3	0.22*		-		Wasielewski[6a]
			4	0.16*	0.04	-		
			5	0.03*		-		
	exTTF[c]	C₆₀	1	-		1.35*		Guldi[10]
			2	-		0.76*	0.01	
			3	-		0.66*		
			5	-		0.54*		
	Zn^{II}TPP[d]	C₆₀	3	0.04*	0.03	0.36*	0.03	Guldi[11]
			5	-0.08*		0.24*		
OPE	Zn^{II}P	Au^{III}P	2	2.0¤		2.9¤		Albinsson[6c, 12]
			3	1.4¤	0.31	2.4¤	0.39	
			4	1.2¤		2.1¤		
			5	1.1¤		2.0¤		
	exTTF[c]	C₆₀	1	-		1.42*		Guldi[13]
			2	-	0.2	1.07*	0.2	
			3	-		0.92*		
ph$_n$	PTZ[e]	PDI[f]	1	2.1*		2.3*		Wasielewski[14]
			2	0.7*		0.8*	0.67	
			3	0.3*	0.46	0.3*		
			4	0.1*		0.07*		
			5	0.05*		-0.04*		
xy$_n$	Ru^{II}	PTZ[e]	2-4	0.45*	0.77			Wenger[6d]
	Re^{I}	PTZ[e]	1-4	0.25*	0.52			Wenger[6d]
fl$_n$	PTZ[e]	PDI[f]	1	0.35*		0.68*		Wasielewski[15]
			2	0.15*		0.36*		
			3	0.01*	0.09	0.16*		
			4	0.15*		0.26*		
	exTTF[c]	C₆₀	1	-0.68*	0.09	-0.02*	0.09	Martìn[16]
			2	-0.61*		-0.05*		
FN$_n$	DMJ-An[g]	NI[h]	1	-0.11*				Wasielewski[17]
			2	-0.05*	0.34			
			3	-0.02*				

[a] Tetracene. [b] Pyromellitimide. [c] Extended Tetrathiafulvalene. [d] Tetraphenylporphyrin. [e] Phenotiazine. [f] Perylene-3,4:9,10-bis(dicarboximide). [g] 3,5-dimethyl-4-(9-anthracenyl)julolidine. [h] Naphthalene-1,8:4,5-bis(dicarboximide).

* Tunneling energy barriers estimated from the donor, acceptor and bridge HOMOs and LUMOs where the HOMO energy levels are approximated to the negative of their oxidation potential, while the LUMO energy levels are given by the difference between the lowest singlet excited state energies E_{00} and the oxidation potentials.

¤ Tunneling energy barriers estimated from excited state energies: ΔE_{CS} is equal to the difference between the donor and bridge E_{00} singlet energies and ΔE_{CR} is equal to the difference between the energy of the charge-separated state and the E_{00}'s of the bridge.

2. Theoretical background

In this section the most essential theoretical framework is presented. It is by no means complete and the interested reader is referred to the any of the excellent text-books on photophysics and electron transfer theory for an in-depth background.

2.1 Photophysics of molecular wires

This tutorial deals with molecules in electronically excited states and the fate of excited states is generally described by the so-called photophysical processes. Typically light energies that correspond to visible or UV light is required to excite a molecule to its lowest electronically excited state. A molecular wire, here defined as a molecule that mediates electronic coupling between its ends, is often a conjugated organic molecule consisting of several subunits linked so that the conjugation extends over a significant part of the molecule. See Table 1 for some examples of molecular wires discussed in this review. When the size of the chromophore grows with increased conjugation, the energy required to reach the lowest excited state decreases. For this reason many molecular wires have low energy absorption bands that are strongly size-dependent both with respect to the excitation energy and molar absorptivity (transition probability).

To act as a molecular wire doesn't at all require the wire to be electronically excited but many of the wire-like properties could be understood through studying excited state properties. Most of the photophysical properties and the description of photophysical transformations such as fluorescence, internal conversion and intersystem crossing, are similar for molecular wires and small organic molecules. There are however some important differences that originate in the degree of delocalization and the fact that excitation energy (excitons) moves quickly over these extended molecular structures. When multiple chromophores are connected, they interact electronically either only through space in case no conjugated structures connect the chromophores or additionally through the conjugated bonds. In many cases, a combination of the two interaction mechanisms contributes to the observed effects that range from slow energy migration to ultrafast delocalization and strong alterations of the electronic spectrum. The through-space interaction, formally between transition dipoles, was quantitatively described by Kasha[18] who gave this weak interaction the name exciton coupling. Even in more strongly interacting molecular wires and assemblies, where the exciton coupling model is quantitatively inadequate, it may still serve as a qualitative tool to discuss how the arrangement of chromophores (the topology) contribute to the properties of the assembly.

2.2 Electron and energy transfer rates

Electron and energy transfer are related phenomena that can be described by a common theoretical framework. Provided that the electronic coupling is very small, the Fermi Golden Rule, eqn (1), predicts the rate of transition between two potential energy surfaces

5

$$k_{if} = (2\pi/\hbar) V_{if}^2 FCWD \tag{1}$$

In this so-called diabatic (non-adiabatic) approximation the electronic coupling, V_{if}, is defined as the effective electronic Hamiltonian matrix element that couples the initial (Ψ_i) and final (Ψ_f) states

$$V_{if} = \langle \Psi_f | H' | \Psi_i \rangle \tag{2}$$

where H' is the operator corresponding to the (small) perturbation mixing the interacting states. The Franck-Condon weighted density of states (*FCWD*) accounts for the conservation of energy and describes the influence from the nuclear modes of the system. Its specific form has to be adapted to the transfer reactions studied. For electron transfer, Marcus approximated the involved potential surfaces by simple parabolas with equal force constants (curvature) which, when combined with transition state theory, leads to:[19]

$$k_{ET} = \sqrt{\frac{\pi}{\hbar^2 k_B T \lambda}} V_{DA}^2 \exp\left(-\frac{(\Delta G^0 + \lambda)^2}{4\lambda k_B T} \right) \tag{3}$$

Fig. 1 illustrates the parameters in eqn (3) where ΔG^0 is the standard free energy change for the electron transfer reaction (energy displacement of the parabolas) and λ is the reorganization energy defined as the potential energy difference between the reactant and product nuclear configurations for the final electronic state, *i.e.* the energy gained by a nuclear (and solvent) relaxation after vertical excitation from the reactant to the product state. For energy transfer reactions the spectral overlap between the involved states can sometimes be estimated from spectroscopic measurements and the *FCWD*-term of eqn (1) is then evaluated from the spectral overlap integral:

$$J = \int I_D(\nu)\varepsilon_A(\nu)d\nu \tag{4}$$

where $I_D(\nu)$ and $\varepsilon_A(\nu)$ are the area normalized emission and absorption spectra of the donor and acceptor, respectively. In the case of energy transfer between triplet states either the emission or absorption spectrum or both are difficult to measure and the rates are therefore often estimated by the approximate Marcus equation (eqn (3)) or the slightly more elaborate Marcus-Jortner equation.[20] In a situation where spectroscopic data are available (e.g. for metal-complexes), however, one should preferably estimate the *FCWD*-factor from the spectral overlap integral (eqn (4)).
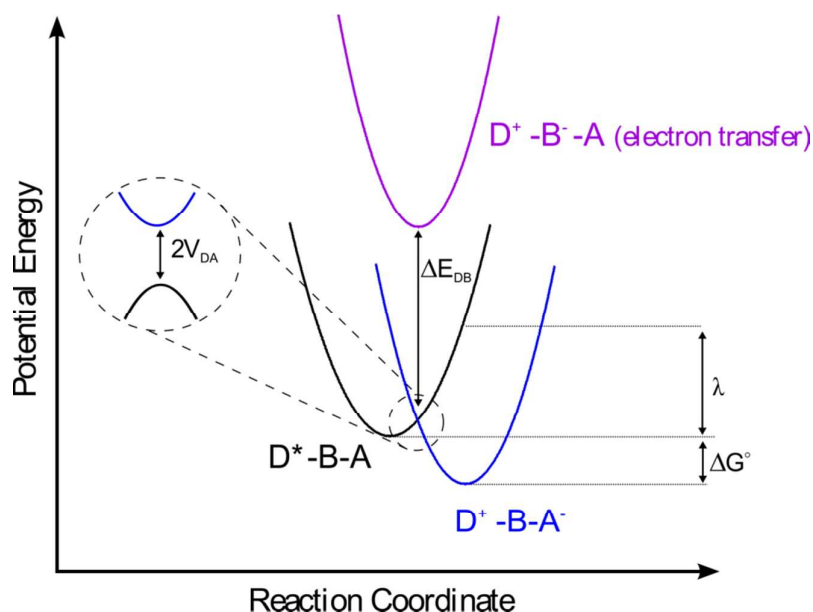
Fig. 1 Potential energy surfaces of the initial excited state D*-B-A, the intermediate reduced bridge state D$^+$-B$^-$-A and the final charge-separated state D$^+$-B-A$^-$. The main factors governing electron transfer in D-B-A systems are also indicated: the driving force $\Delta G°$, the reorganization energy λ, the electronic coupling V_{DA} and the tunneling energy barrier ΔE_{DB}.

2.3 Distance dependence – mechanisms for electron transfer

Electron transfer between ends of a molecular wire is dictated by either of two mechanisms; the coherent tunneling or incoherent hopping mechanism (Fig. 2). The tunneling mechanism is often described by the superexchange model (*vide infra*) which requires the donor and acceptors at either ends of the wire to be energetically well separated from the bridge states.[4] One important consequence is that the bridge is never either reduced or oxidized but merely functions as a coupling medium for the transfer process. In contrast, the incoherent hopping mechanism involves real intermediate states that actively transport the electron or hole along the wire. This is why the incoherent mechanism often is called thermally activated hopping.[21] In many real cases the transfer is expected to be governed by a mixture of the two mechanisms and experimentally this has been observed by several groups.[22]

The coherent tunneling mechanism is, in absence of a Coulomb interaction, dominated by the exchange interaction that governs the distance dependence of the rates for both electron and triplet energy transfer (and in some cases also singlet energy transfer). For this mechanism, the distance dependence of the observed electron transfer rates is approximately exponential:

$$k = k_0 \exp\left(-\beta R_{DA}\right) \tag{5}$$

where R_{DA} is the distance between the donor and acceptor (measured along the wire – not through space), k_0 the limiting rate at donor-acceptor contact, and β is the system specific attenuation factor. Triplet energy transfer rates also have exponential distance dependence but with attenuation factor

equal to 2β as discussed in section 4. Numerous experimental and computational studies have verified eqn (5) and β-values for a wide range of molecular wires (molecular bridges) have been determined. In general, β-values are larger for systems comprised of σ-bonds than for systems connected by π-conjugated bridges, which gives more efficient long-range transfer of electrons or excitation energy. Although β-values only apply for mechanisms that are expected to decay exponentially (eqn (5)) they have been used as quality factors also for electron transfer that occur via the incoherent hopping mechanism. As an empirical measure for the attenuation of the rate vs. distance this is acceptable but since hopping is not expected to decay exponentially it could be quite confusing when comparing β-values with the purpose of trying to understand the mechanistic differences between hopping and long range tunneling.
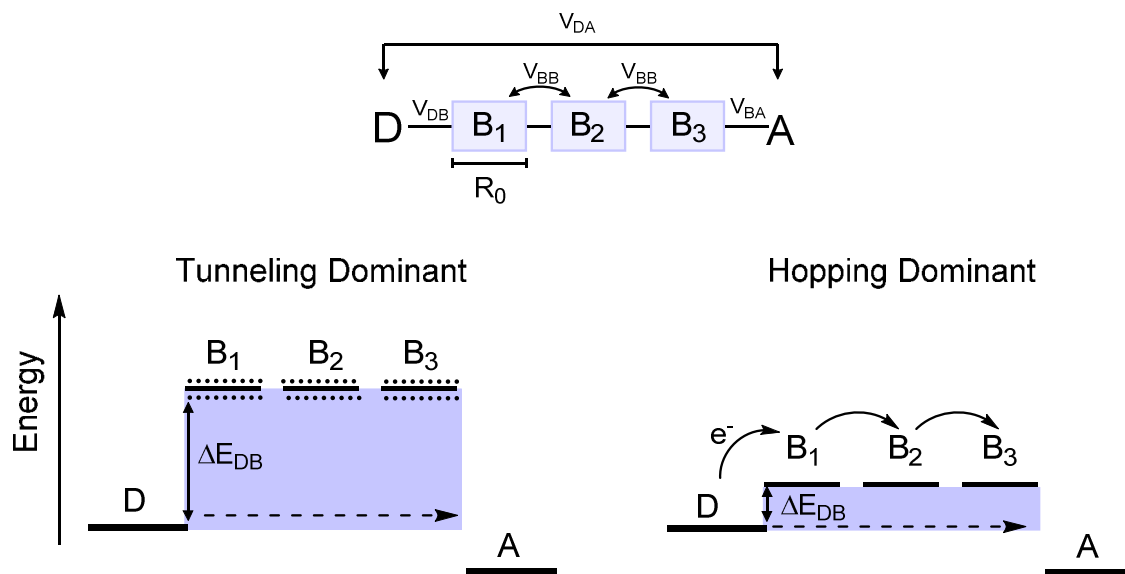
2.4 Superexchange model

For the coherent tunneling mechanism the influence of the intervening medium has been described by the so-called superexchange model.[4] In this model the magnitude of the electronic coupling is given by a first-order perturbation theory treatment as:

$$V_{DA} = \frac{V_{DB}V_{BA}}{\Delta E_{DB}} \left(\frac{V_{BB}}{\Delta E_{DB}} \right)^{n-1} \tag{6}$$

Eqn (6) gives the total electronic coupling (V_{DA}) in terms of the electronic coupling of the bridge to the donor and acceptor (V_{DB} and V_{BA}), the interaction, V_{BB}, between nearest neighbors of a chain composed of n identical units, and the energy gap, ΔE_{DB}, between the relevant donor and bridge localized states (Fig. 2). If the length of the chain connecting the donor and acceptor is directly proportional to n, *i.e.* $R_{DA} = nR_0$, where R_0 is the length of one subunit and the electronic coupling between subunits is small compared to the energy gap ($V_{BB}/\Delta E_{DB} \ll 1$), the distance dependence of the electronic coupling, and therefore also the rate, is exponential. Within this approximation the attenuation factor β is given by eqn (7).

$$\beta = \frac{2}{R_0} \ln \left| \frac{\Delta E_{DB}}{V_{BB}} \right| \tag{7}$$

If the bridge is treated as a single chromophore, i.e. a single repeating unit, eqn (6) is simplified to $V_{DA} = V_{DB}V_{BA}/\Delta$ that clearly shows the reciprocal energy gap dependence of the electronic coupling as will be discussed in the following sections.[12a, 23]

Fig. 2 Schematic comparison of the tunneling (left) and hopping (right) mechanisms in a D-B-A system here shown for electron transfer. The McConnell superexchange model for electron tunneling through molecular structures is illustrated in the top drawing. For the tunneling model, the bridge virtual states are represented as dashed lines; while in the hopping model, the local bridge states are drawn as solid lines. ΔE_{DB} represents the tunneling energy barrier for electron injection onto the bridge.

3. Tunneling energy gap effects in π-conjugated D-B-A systems

The large interest in π-conjugated bridges arises from their ability to mediate electron transfer over long distances. To evaluate the efficiency of electron transfer over distance, one commonly determines the distance-dependence of the electron/hole transfer through the bridge in a D-B-A system. In practice, the transfer rate constants, k_{ET}, are measured for different donor-acceptor distances R_{DA}, achieved by simply varying the number of rigid bridge units separating the donor and acceptor. Results of this distance-dependence are then presented in a logarithm plot of k_{ET} versus R_{DA}. As predicted by the McConnell model (eqn (5)), the transfer rates k_{ET} are expected to display exponential distance dependence; in other words, in a semi-logarithmic scale the transfer rate constants should describe a straight line with a slope corresponding to the attenuation factor, -β. Table 1 provides the measured β-values of some typical D-B-A systems. These attenuation factors could vary quite substantially for different bridges, and ideally a value as close to zero as possible that would allow charge transport over almost "infinite" distances would be preferable. However, if the electronic coupling gets very large leading to very small β-value the distance dependence is no longer well described by the McConnell model and is no longer expected to decay exponentially. In Table 1, one can note substantial variations of the β-values between the different π-conjugated bridges, and at first the β-values could seem to be quite random and difficult to predict. Another important feature to

notice is the different β-values reported for the same bridge when used with different donor/acceptor couples.

Although initially seen as a simple and inactive spectator of the charge transfer process, it is now evident and quite well understood that the bridge does influence the electron transfer. According to the McConnell model (eqn (7)), three factors come in the expression of the attenuation factor β: the tunneling energy gap ΔE_{DB}, the electronic coupling between individual bridge units, V_{BB}, and the size of the individual bridge units, R_0. Among these three factors, the most critical parameter is the tunneling energy gap, ΔE_{DB}. Direct experimental evidence of the tunneling energy gap effect has been lacking for a long time due to the fact that ΔE_{DB} is a vertical energy barrier at the transition state, a quantity which is not easily accessible (Fig.1). In the last ten years, much effort has been put in the design of experiments enabling to test theoretical predictions. Several studies have appeared in the literature providing clear experimental evidence of the influence of bridge energetics on charge transport in D-B-A systems.[6a, 6d, 12a, 24] From these studies, the wide range of β-values seen in Table 1 could be ascribed in part to substantial differences in the tunneling energy gap between the different D-B-A systems.

The tunneling energy gap effect was first demonstrated by Wasielewski and co-workers. They investigated the distance dependence of electron transfer rates in a series of OPV-bridged D-B-A systems, with tetracene as donor and pyromellitimide (PI) as acceptor (see Table 1).[6a, 24] For both charge separation (CS) and recombination (CR), they measured the transfer rates (k_{CS} and k_{CR}) and plotted them as function of R_{DA} on a semi-logarithmic scale. While the data points for charge separation in the shorter members (n = 1, 2) fell into a single line in agreement with a tunneling mechanism, the longer members of the series (n = 3-5) deviated strongly from this line and showed faster rates and weak distance dependence. This *"irregularity"* in the distance dependence was interpreted as the result of a change in charge transport mechanism. While for the shorter bridges (n = 1, 2), charge transport occurs via superexchange tunneling, bridge-assisted electron hopping predominates in the longer bridges (n = 3-5). For the charge recombination, a similar mechanism change was observed for n = 5. As the same donor/acceptor couple was used throughout the entire series, this crossover from tunneling to hopping could only be related to properties of the bridge. Indeed for this particular bridge, increasing the bridge length also increases the size of the conjugated system and consequently the energy of the bridges states, essentially the HOMO-LUMO gap, decreases. This leads to a decrease of the energy gap between the LUMO of the donor and the LUMO of the bridge, and hence a decrease of the tunneling energy barrier. In the longer members of this OPV-bridged series, ΔE_{DB} is small enough that reduction of the bridge becomes possible. Charge can migrate between the donor and the acceptor in a multistep fashion, first moving from the donor to the bridge, and then from the bridge to the acceptor. This first example shows that in distance-dependence studies both the width (R_{DA}) and the height (ΔE_{DB}) of the tunneling energy barrier may vary simultaneously, making the interpretation of the results more intricate. Thus, when studying charge

transport in D-B-A molecules with π-conjugated bridges, it may be desirable to vary a single parameter at a time, either the width or the height of the tunneling barrier. In this aim, two approaches have been proposed to solely focus on a single parameter.

### 3.1 Using structurally identical bridges

In this first approach, one compares the transfer rates of a series of D-B-A molecules with constant R_{DA}, that consists of the same donor/acceptor couple connected by structurally similar but electronically different bridge molecules. Albinsson and co-workers have used this approach and designed one series of D-B-A systems ZnP-RB-AuP$^+$ where RB denotes an OPE-based bridge (Fig. 3). For the entire series, ZnP acts as an electron donor while AuP+ is the electron acceptor.[6c, 12a] The electronic structure of the OPE bridge (3B) could be modified by replacing the central benzene unit by either naphathalene (NB) or anthracene (AB). This allowed varying the tunneling energy barrier for charge separation ΔE_{CS} and recombination ΔE_{CR} while keeping a fixed R_{DA}. Fig. 3 provides schematic energy diagrams for the three D-B-A systems with their respective tunneling energy gaps ΔE_{CS} and ΔE_{CR} for charge separation (CS) and recombination (CR), respectively. Note that the tunneling energy gaps are not the true energy barriers but are approximations from the donor-acceptor LUMOs. In the present case, photo-excitation of the donor involves a close to pure HOMO-LUMO transition; hence the LUMOs of both donor and bridge could be directly related to the energy of their first singlet excited states (E_{00}). Thus the tunneling energy barriers ΔE_{CS} and ΔE_{CR} were calculated as the energy difference between the donor and bridge E_{00} singlet excited states energies, and as the energy difference between the charge-separated state and the first singlet excited state of the bridge, respectively. Moving from benzene (3B) to naphthalene (NB) to anthracene (AB), i.e. to lower lying singlet excited states on the bridging unit, leads to a decreased tunneling energy gap. This decrease in ΔE_{CS} and ΔE_{CR} was reflected very well in the observed electron transfer rates, which increased when going from benzene (3B) to naphthalene (NB) to anthracene (AB).
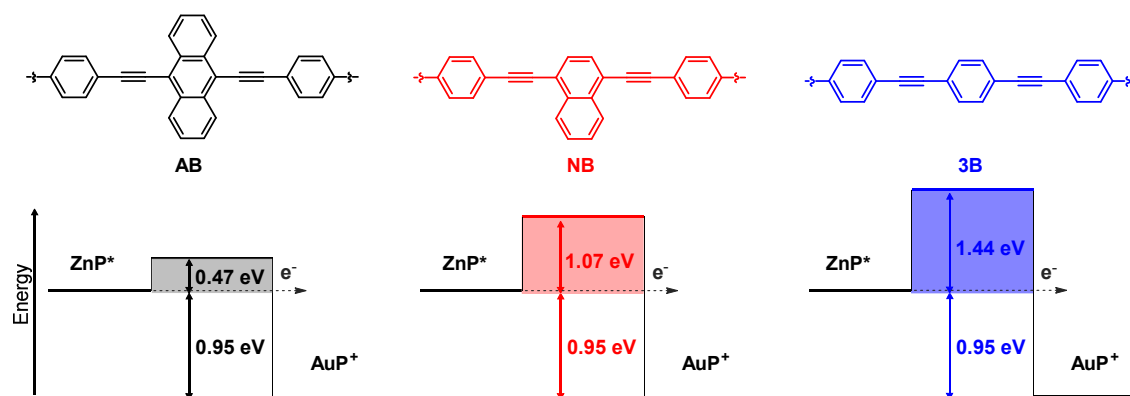
Fig. 3 (top) Molecular structures of the D-B-A systems ZnP-RB-AuP$^+$ with RB = AB (black), NB (red) and 3B (blue). The edge to edge donor-acceptor distance was 19.6 Å in the three D-B-A systems.

(bottom) Schematic energy diagrams for charge separation via electron transfer in these systems. Adapted from references [6c, 12a].

The solvent dependence of the electron transfer rates for both charge separation and recombination processes were also investigated. The transfer rates were measured in six solvents with different polarity using both steady-state and time-resolved fluorescence. Along with estimates of the driving forces $(\Delta G°)$ and reorganization energies (λ) accompanying charge separation and recombination, these measurements gave indirectly access to the electronic coupling, V_{DA}. Indeed, in a plot of ln $(k_{ET}\lambda^{1/2})$ against $(\Delta G°+\lambda)^2/(4\lambda k_B T)$ the data could be successfully fit to a straight line with a slope of -1 in agreement with the linearized Marcus equation (eqn (3)). Further, the overall donor-acceptor coupling for the three different bridge systems could be estimated from the intercept of the fitting curves. Finally, the key finding of this work was the experimental demonstration of the linear correlation between the electronic coupling and the inverse of the tunneling energy gaps, $1/\Delta E_{CS}$ or $1/\Delta E_{CR}$, (Fig. 4) as predicted by the McConnell model.
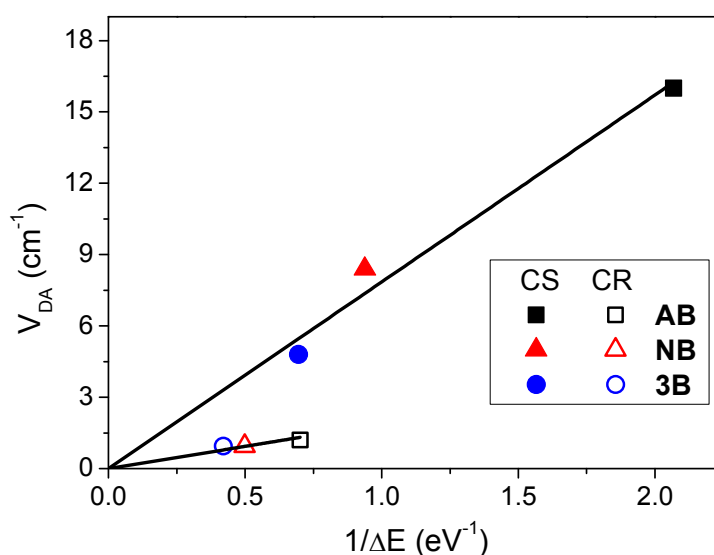
Fig. 4 Electronic coupling, V_{DA} versus the inverse of the energy gap, ΔE, for charge separation (filled symbols) and charge recombination (empty symbols) in the series ZnP-RB-AuP$^+$ with R = AB (black), R = NB (red) and R = 3B (blue). The lines are linear fits obtained when fixing the intercepts $V_{DA}(0) = 0$. Adapted from reference [12b].

As an extension, the distance dependence of the electron transfer rates was studied in the series ZnP-nB-AuP$^+$ where n the number of OPE units varied between 2 to 5, spanning edge-to-edge donor-acceptor distances, R_{ee}, between 13 and 33 Å.[6c, 12b] On a semi-logarithmic plot, the transfer rates $ln\ k$ against R_{ee} described a straight line, in line with a tunneling charge transport (Fig. 5). From the slopes of the curves, the attenuation factor β was estimated to 0.31 Å^{-1} for charge separation and 0.39 Å^{-1} for

charge recombination. These different β-values reflected once more tunneling energy gap effects with $\Delta E_{CS} < \Delta E_{CR}$ (see Fig. 4, as an example for the trimer ZnP-3B-AuP$^+$, crude estimates of the barrier heights give: $\Delta E_{CS} \approx 1.4$ eV $< \Delta E_{CR} \approx 2.4$ eV). It can be interesting to compare the behavior of OPE-bridged D-B-A molecules with the one of OPV-bridged D-B-A molecules discussed earlier. As for OPV-bridged D-B-A systems, when the OPE bridge gets longer, the tunneling energy barriers ΔE_{CS} and ΔE_{CR} decrease due to increased conjugation. In OPV-bridged D-B-A molecules, we saw that variation of the tunneling energy barrier led to a change in charge transport mechanism. Here in this particular OPE-bridged series no deviation from the exponential distance-dependence was observed. This indicates that the tunneling energy barrier remains large enough for charge transport to occur via tunneling even for the longer members of the series. In other words, the distance dependence of the electron transfer rates in the ZnP-nB-AuP$^+$ series results mainly from changes in the barrier width (n or R_{ee}) and to a smaller degree in its height (ΔE_{CS} and ΔE_{CR}).
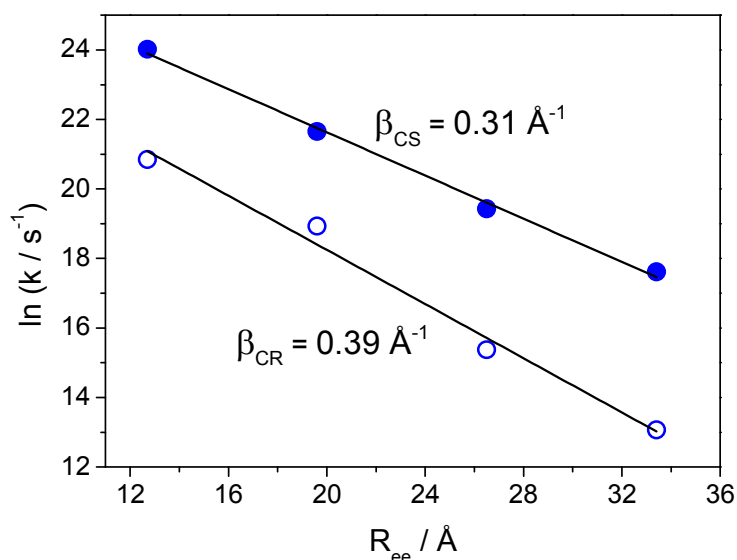
Fig. 5 Distance dependence of the charge separation ($\bullet$) and charge recombination ($\circ$) rates in the D-B-A series ZnP-nB-AuP$^+$ with the number of OPE units n = 2-5. Adapted from reference [12b].

A more recent study comparing charge transport in structurally similar bridges is the work of Wenger et al. on D-B-A molecules linked by phenylene-based bridges.[25] They investigated hole tunneling in D-B-A systems with a rhenium (I) complex as hole donor and phenothiazine as hole acceptor. The donor/acceptor couple was connected either by two phenyls (ph$_2$), two xylene groups (xy$_2$) or a fluorene group (fl$_1$) (see Table 1). Again despite the different bridge structure, the donor-acceptor separation remains identical in the three D-B-A systems. Transient absorption measurements revealed an increase in the hole transfer rates when going from phenylene ($k_{HT}= 0.5\ 10^8\ \text{s}^{-1}$) to xylene ($k_{HT} = 2.6\ 10^8\ \text{s}^{-1}$) and fluorene ($k_{HT} = 5.3\ 10^8\ \text{s}^{-1}$). In parallel, they also estimated the hole tunneling energy gap

13

from the redox potentials for the different bridge structures: ΔE_{DB} = 0.54 eV for ph$_2$, ΔE_{DB} = 0.25 eV for xy$_2$ and ΔE_{DB} = 0.16 eV for fl$_1$. The faster transfer rate observed for the fluorene bridge (fl$_1$) reflects nicely the smaller tunneling energy barrier. However the phenylene-bridged D-B-A system, which shows an intermediate transfer rate, has also the highest tunneling energy barrier ΔE_{DB}. The tunneling energy gap argument does not solely explain all the kinetic data. When going from phenylene to xylene to fluorene, the average torsional angle, $\varphi_{Ph\text{-}Ph}$, between the two phenyl planes also varies and decreases from 65° for xy$_2$ to 35° for Ph$_2$ to 6° for fl$_1$. This results in increasing the internal bridge electronic coupling, V_{BB}, and thereby increasing the overall electronic coupling, V_{DA} (eqn (6)), when going from xylene via phenylene to fluorene bridge units. Thus, the faster rate in the fluorene-bridged D-B-A system presumably results from the combined effect of a smaller tunneling energy barrier ΔE_{DB} and a stronger internal bridge coupling (lower $\varphi_{ph\text{-}ph}$). For the phenylene-bridged D-B-A system the intermediate V_{BB} may compensate for the larger tunneling energy barrier ΔE_{DB}, leading to an intermediate transfer rate.

3.2 Using bridges with length-independent (redox) energies

A second approach to study solely the influence of the width of the tunneling barrier is to use D-B-A systems in which the bridge energetics are independent of the bridge length. Thanks to a combined effort of synthetic and physical chemists, several examples of π-conjugated systems with length-independent bridge redox potentials have recently appeared in the literature. Oligo-fluorene (fl$_n$), oligo-fluorenone (FN$_n$) and oligo-p-xylenes (xy$_n$) are examples of π-conjugated systems which show nearly length independent redox potentials.[15a, 17, 26] In two separate studies, Wasielewski and co-workers investigated photoinduced electron transfer in D-B-A molecules, bridged by either oligo-fluorenes[15a] or oligo-fluorenone[17] (see Table 1). However, both D-B-A series revealed to be less interesting for investigating electron tunneling as a hopping mechanism dominated the charge transport (see the next chapter for a more detailed discussion). In contrast, charge transport in oligo-p-xylene-bridged D-B-A molecules occurs essentially via electron tunneling. In a nice series of papers, Wenger and co-workers demonstrate that xylene-bridged D-B-A molecules are interesting model systems to isolate the effects of width or height of the tunneling barrier on long-range charge transfer.[6d] They designed two series of xylene-bridged D-B-A molecules and measured the distance-dependent hole transfer rates by varying the number of xylene bridge units (see Table 1). In the first series, the donor/acceptor couple was phenothiazine (PTZ) and rhenium tricarbonyl phenanthroline (Re(I)). In the second series, they employed a different donor/acceptor couple with again phenothiazine (PTZ) as donor but ruthenium(II)tris(2,2´-bypridine) (Ru (II)) as acceptor. In both the PTZ-xy$_n$-Re (n = 1-4) and PTZ-xy$_n$-Ru series (n = 1-4), the absorption spectra remain close-to-identical upon lengthening of the bridge, indicating that the bridge excited states and thereby the tunneling energy gap is length-independent for both series. In accordance with the superexchange theory, the hole transfer rates decreased exponentially with the donor-acceptor distance in both series,

confirming hole tunneling as the dominant charge transport mechanism. However they determined significantly different attenuation factors with $\beta = 0.52$ Å^{-1} for PTZ-xy$_n$-Re and $\beta = 0.77$ Å^{-1} for PTZ-xy$_n$-Ru. The different β-values could be ascribed to differences in tunneling energy barriers between the two series, that arise from the different acceptor used: ΔE_{BA}=0.25 eV for PTZ-xy$_n$-Re and ΔE_{BA}=0.45 eV for PTZ-xy$_n$-Ru. Finally this experimentally demonstrates that the β-value is specific to the donor-bridge-acceptor ensemble and not solely to the bridge unit.

3.3 Crossover from tunneling to hopping

When the tunneling energy gap (ΔE_{DB} or ΔE_{BA}) is small enough, i.e. the bridge and donor (or acceptor) states are nearly resonant, the bridge reduced (or oxidized) states become thermally accessible. Charge transport occurs then predominantly via incoherent hopping. This means that the electron (or hole) resides temporarily on the bridge before reaching the electron acceptor (or donor). Thus a clear and simple evidence of incoherent charge hopping is often the detection of the bridge reduced transient state D$^+$-B$^-$-A (or oxidized transient state D-B$^+$-A$^-$) prior to formation of the fully charge-separated state in transient absorption experiments. As the bridge transient species are often very short lived (below the time resolution of transient absorption measurements), deviations from the exponential distance dependence of the transfer rates have also been used as indicator of incoherent charge hopping. Indeed for incoherent hopping, the distance dependence of the transfer rates is not anymore exponential or ruled by the superexchange (McConnell) theory, and generally very weak distance dependence is observed. Over the last twenty years, several examples of D-B-A molecules with π-conjugated bridges showing "irregular" distance dependence of their transfer rates attributed to a switch from tunneling to hopping charge transport have been reported in the literature. The large interest in D-B-A systems with charge transport occurring in the hopping regime resides in the low distance dependence of charge transport, hence the ability of mediating charge over much longer distances than in the tunneling regime. In the literature, these D-B-A systems have often been qualified as "wire-like". Crossover from tunneling to hopping and the appearance of a wire-like behavior has been first observed by Wasielewski and co-workers in OPV-bridged D-B-A molecules with a tetracene donor and a pyromellitimide acceptor, as described above.[6a] In an analogous work on oligophenylene-bridged D-B-A systems, they observed a similar switch from tunneling to hopping when increasing the number of phenyl bridge units between the donor (PTZ) and acceptor (PDI), see Table 1.[14] Once more, this was evidenced by a non-exponential distance dependence of the transfer rates. Like the OPV-based bridges, oligophenylene bridges possess strongly length-dependent HOMO-LUMO gaps resulting in a tunneling energy barrier for this D-B-A system, that varies between 2.1 eV (n = 1) and 0.05 eV (n = 5) for charge separation and between 2.3 eV and -0.04 eV for charge recombination (Table 1). Thus for the longer members (n = 4, 5), the tunneling energy barriers are small enough that population of the bridge states might occur and incoherent hopping dominates the charge transport. Additionally, they measured electron paramagnetic resonance (EPR) spectra and

estimated the magnitude of the spin-spin exchange interaction (2J) through the entire series, a quantity which is proportional to the donor/acceptor coupling V_{DA}. As for the electron transfer rate constants, they observed an exponential distance dependence of the spin-spin exchange interaction 2J only up to n = 4, supporting their conclusion of a change in the charge transport mechanism in the longer system with n = 5. Using the same donor/acceptor couple (PDI/PTZ), Wasielewski and co-workers have also designed a series of D-B-A molecules, bridged by oligofluorene (fl_n) with n = 1-4. As mentioned earlier, fluorene bridges (fl_n) with n ≥ 2 possess nearly length-independent redox potentials hence the tunneling energy barrier remains almost constant for PDI-fl_n-PTZ with n ≥ 2. Of much interest in this particular system is the matching of the acceptor and bridge energy levels which is achieved for n= 2-4. This results in incoherent hopping hole transport with a very small β-value ($\beta = 0.093$ Å^{-1}) and gives rise to a "wire-like" behavior of the fluorene bridges in the PDI-fl_n-PTZ systems.
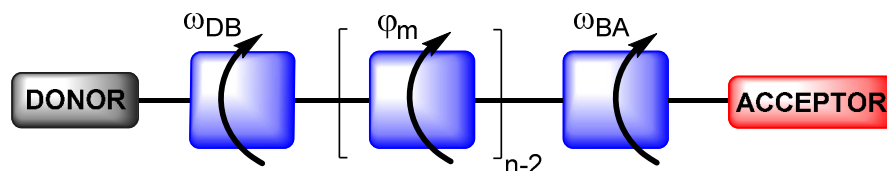
In both examples, we have seen that wire-like charge transport is achieved by matching the donor (or acceptor) and bridge energy levels. This promotes incoherent hopping charge transport and precludes the strongly-distance dependent tunneling charge transport to occur. However in a recent paper, Wasielewski and co-workers reported a high β-value for hole transfer together with evidence of a hopping mechanism in fluorenone-bridged D-B-A systems (see Table 1).[17] In these particular D-B-A systems, the selected donor (DMJ-An), bridge (FN_n) and acceptor (NI) give rise to a stepwise downhill energy gradient within the D-B-A molecule. Surprisingly, even though the downhill energy gradient in DMJ-An-FN_n-NI (n = 1-3), they observed an exponential distance dependence of the transfer rate with a large attenuation factor, $\beta = 0.34$ Å^{-1}. Such large attenuation factor would normally be expected for charge transport in the tunneling regime. However femtosecond transient absorption measurements confirmed the formation of the intermediate bridge reduced states DMJ$^+$-An-$FN_n$$^-$NI, supporting their conclusion of a hopping mechanism. The unusual distance dependence in the hopping regime was rationalized by invoking the push-pull character of the DMJ-An donor, which forms upon photo-excitation a primary charge-separated state DMJ$^+$-An$^-$. The electrostatic attraction between the two charges slows down both the electron injection onto the bridge and the subsequent electron hopping, resulting in the high attenuation factor observed. This work demonstrates that a stepwise downhill energy gradient in a D-B-A molecule does not necessarily imply a "wire-like" behavior of the bridge. It also shows that the attenuation factor β is not a reliable indicator to distinguish between tunneling and hopping charge transport.

4. Conformational effects on electron transfer processes in π-conjugated systems

So far we have described a quite simple picture of the factors influencing electronic mediation in D-B-A systems in which the tunneling energy barrier and width are the only factors governing the distance dependence and the nature of charge transport (i.e. coherent tunneling or incoherent hopping). In

reality, conformational dynamics of the bridge, temperature and solvent may affect the donor/acceptor electronic communication hence the measured transfer rates in D-B-A systems. This generally complicates the picture, and renders the prediction and interpretation of the transfer rates quite difficult. The following discussion is restricted to the influence of the bridge conformation on charge transport in D-B-A molecules. Although solvent parameters influence the electron transfer rate through the reorganization energy λ and driving force $\Delta G°$ (eqn(3)), in the interest of clarity we will refrain from discussing these factors here.
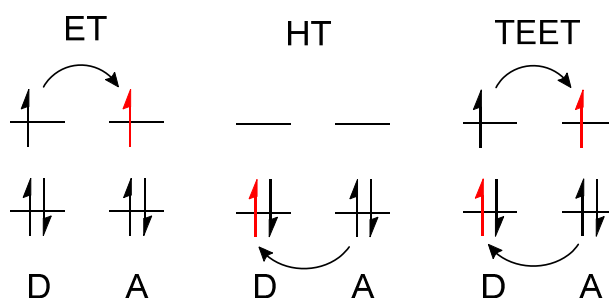
In the previous discussion, the bridge was considered as a rigid structure. However the bridge is a dynamic entity, in which each unit may rotate, giving rise to different conformations. The conformational dynamics of the bridge is both temperature and solvent dependent. This influences the bridge energetics and thereby the tunneling energy barriers in D-B-A systems. Furthermore, variations in the dihedral angles between individual units within the bridge and between the bridge and the donor or acceptor might strongly modulate the overall donor/acceptor electronic coupling. Several experimental and theoretical studies have shown that in D-B-A systems linked by a series of planar π-conjugated bridge units, the dihedral angles between individual units are the major conformational parameters modulating the electronic coupling. In systems where the donor and acceptor are planar conjugated molecules and the bridge is constituted by a series of planar molecular subunits (see Table 1), one generally defines two sets of dihedral angles (Fig. 6): the dihedral angle between the donor or acceptor plane and the plane of the first bridge unit denoted ω_{DB} and ω_{BA}, respectively, and the dihedral angles between the planes of two consecutive bridge units denoted φ_m with m=1,2...n-2 where n is the number of bridge units.

Fig. 6 Schematic showing the dihedral angles used to describe conformational dynamics effects in a D-B-A molecule consisting of planar molecular subunits.

Influence of the bridge conformation (i.e. dihedral angles ω_{DB}, φ, ω_{BA}) on the electronic coupling, V_{DA}, has been shown experimentally for intramolecular triplet excitation energy transfer (TEET) but not for electron transfer (ET), although theoretically predicted.[27] One reason for this lack of experimental data is the difficulties to produce a series of D-B-A systems in which one can vary the orientation of the bridge without simultaneously vary any bridge energetics such as the tunneling energy barrier for electron transfer.[14b, 28] In principle, one can estimate the electronic coupling from the measured transfer rates obtained for the different conformations using the Fermi Golden Rule (eqn (1)). In the case of

ET, evaluation of the Franck-Condon weighted density of states (FCWD) requires to calculate the standard free energy change ΔG^0 and the reorganization energy λ (eqn (3)). For TEET, the rate for triplet energy transfer k_{TEET} can also be expressed using the Fermi Golden Rule if the donor/acceptor coupling V_{DA} is weak. But in contrast to ET, the FWCD is simply given by the spectral overlap of the emission spectra of the donor and acceptor (eqn (4)). The electronic coupling is then the only remaining unknown in eqn (1) and can be obtained from the measured kinetic data. Another advantage of TEET measurements is the minimal influence of solvent effects due to the absence of charge movement. Finally, qualitative results from TEET studies are expected to prevail for ET, as TEET is also an electron exchange phenomena that can be viewed as two simultaneous ET reactions (Fig. 7). This qualitative argument was supported by the work of Closs et al. who experimentally demonstrated the connection between the electronic coupling for triplet energy transfer and electron and hole transfer for saturated bridges: $|V_{TEET}|=\text{const}|V_{ET}||V_{HT}|$.[29]
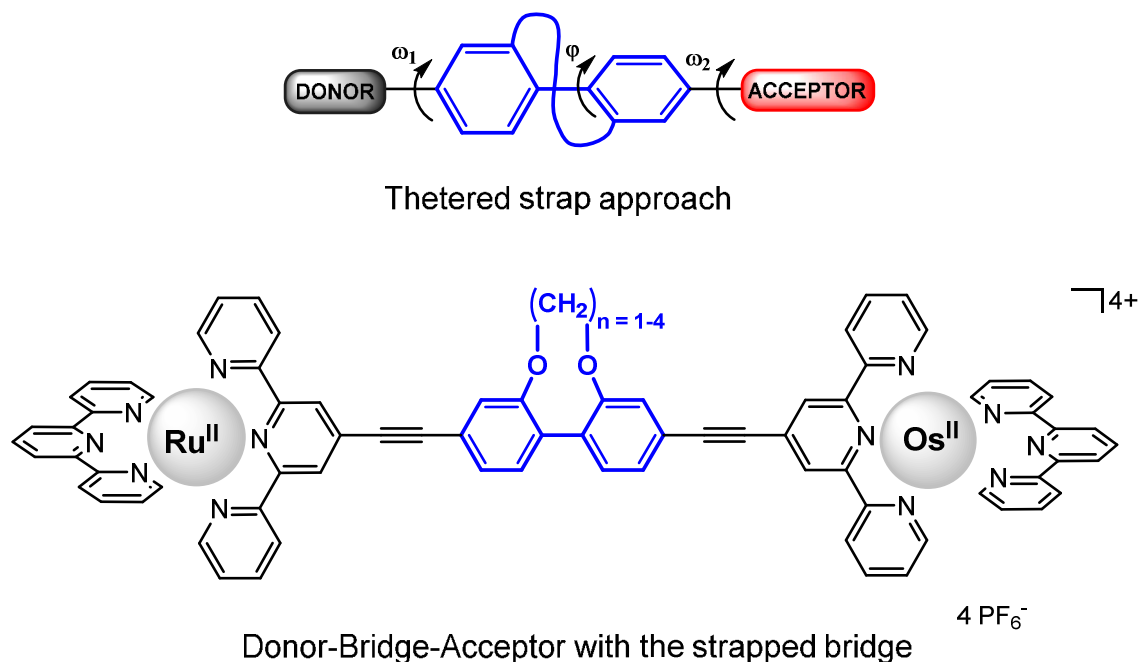

Fig. 7 Schematic of the triplet excitation energy transfer (TEET) between a donor and an acceptor, as a simultaneous electron and hole transfer reaction. Adapted from reference [29].

4.1 Geometric control of the electronic coupling

Among the first to show experimentally the influence of the bridge conformation on the donor/acceptor electronic coupling in D-B-A systems was Harriman and co-workers.[30] They probed the effect of torsional angles within the bridge structure on the rate of intramolecular triplet excitation energy transfer k_{TEET} in a series of ruthenium (II)/osmium (II) (tpy)$_2$ donor/acceptor complexes linked by ethynylene-substituted biphenyl bridges. They could control and tune the dihedral angle between the phenyl units, $\varphi_{Ph\text{-}Ph}$, by attaching a tethering strap between the two phenyl units and varying the number of carbon atoms in the strap (Fig. 8). This gave access to a wide range of dihedral angles while keeping a fixed donor-acceptor distance. To prevent any undesirable rotation to occur, triplet energy transfer rates were measured in a low temperature organic glass matrix, thus maintaining the bridge frozen into its lowest-energy conformation. Their results showed a pronounced conformational dependence of the transfer rates, hence of the electronic coupling which was largest when the phenyl units were close to coplanar ($\varphi = 30°$). At the largest dihedral angle ($\varphi = 90°$), the electronic coupling V_{TEET} decreased drastically, resulting in a measured transfer rate k_{TEET} that decreased by a factor of 80.

Furthermore, they demonstrated experimentally the quadratic dependence of the electronic coupling with the overlap integral between two π-orbitals: $V_{TEET}(\varphi) = V_{ET}(\varphi)V_{HT}(\varphi) = \cos^2(\varphi)$.

Thetered strap approach
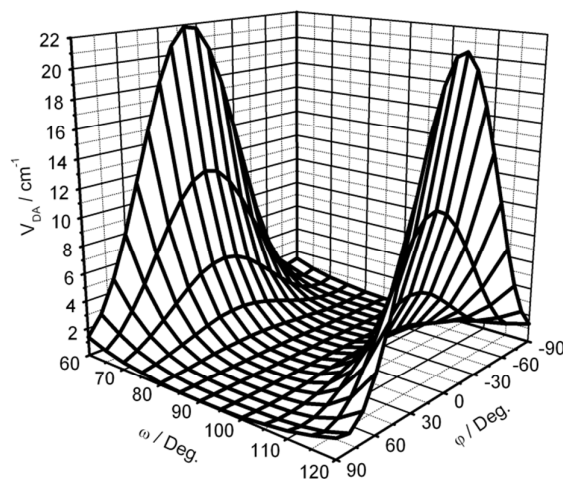

Donor-Bridge-Acceptor with the strapped bridge

Fig. 8 (top) Schematic of the tethered strap approach used to tune the dihedral angle, φ, between the planes of the two consecutive phenyl bridge units. Adapted from ref [7a]. **(bottom)** Molecular structure of one D-B-A system employing the tethered strapped bridge studied by Harriman and co-workers.[30]

4.2 Temperature control of the bridge conformational distribution

Another approach to investigate how bridge conformation affects the flow of excitation energy or electrons between the donor and acceptor in D-B-A systems is to use temperature as a way to tune the Boltzmann distribution of conformations. At first this approach seems more accessible, since it is less challenging in terms of synthesis. However, interpretation of the temperature-dependent transfer rates is a challenge as several parameters are affected simultaneously by temperature. Firstly, temperature impacts several properties of the solvent, such as the dielectric constant and the refractive index which influence the driving force $\Delta G°$ and reorganization energy λ for the electron transfer rate (eqn (3)). Thus as stated above, it is easier to study temperature dependence of TEET as to minimize the solvent-induced effects. Secondly, another temperature dependent property of the solvent is its viscosity that increases as the temperature decreases, hence slowing down rotations of the molecular planes within the bridge structure.

Albinsson and co-workers have investigated the temperature dependence of TEET, both experimentally and theoretically, in a series of donor-acceptor systems linked by OPE bridges, ZnP-nB-H$_2$P with n = 2-5.[31] The distance-dependent transfer rates, k_{TEET}, were measured for temperatures between room temperature and 80 K. As for ET, in line with the McConnell model, the transfer rates

showed exponential distance dependence for the entire temperature range, but more interestingly the attenuation factor, β, was found to be temperature dependent. In parallel to these experiments, a theoretical model was derived to calculate the total electronic coupling, V_{DA}, based on a Boltzmann distribution of the bridge conformations.[32] This model demonstrates the conformational gating of the electronic coupling, and hence of the attenuation factor β. The procedure involved density functional theory (DFT: B3LYP/6-31G*) calculations of the potential energy surfaces as function of the dihedral angles ω, $\Sigma\varphi_m$ (Fig. 6) followed by calculation of the total electronic coupling V_{DA} for each conformational distribution (i.e. each set of ω, $\Sigma\varphi_m$ values). V_{DA} can be derived from half the triplet excitation energy difference (calculated with time dependent (TD)-DFT) between the two lowest triplet excited states at the avoided crossing geometry (Fig. 1). In an unsymmetrical system such as here ZnP-nB-H_2P, finding this crossing point is not straightforward and can be quite complex. Thus, to simplify the procedure, the electronic coupling for the corresponding symmetrical systems, ZnP-nB-ZnP (n = 2-5) was calculated. Fig. 9 illustrates the variation of the total electronic coupling V_{DA} for ZnP-2B-ZnP as function of the two dihedral angles $\omega = \omega_{DB} = -\omega_{BA}$ and φ. Again the $\cos^2\varphi$ dependence of the electronic coupling is nicely demonstrated. The electronic coupling V_{DA} reaches a maximum when both phenyl planes are coplanar ($\varphi = 0°$) and a minimum when both dihedral angles φ and ω equal 90° (i.e. all molecular planes in ZnP-2B-ZnP are orthogonal to each other). This shows the possibility of using conformational changes to tune the electronic coupling.

Fig. 9 Calculated electronic coupling for TEET, V_{DA}, for the symmetric system ZnP-2B-ZnP as function of both porphyrin-bridge (ω) and phenyl-phenyl (φ) dihedral angles. Reprinted with permission from [32b]. Copyright 2006 American Chemical Society.

The total electronic coupling V_{DA} can be expressed as a product of one-parameter functions: $V_{DA}(\omega_1, \varphi_1, \varphi_2,...,\varphi_{n-1}, \omega_2) = V(\omega_1)V(\varphi_1)V(\varphi_2)...V(\varphi_{n-1})V(\omega_2)$. By introducing a Boltzmann-weighted

contribution for each conformational configuration, the impact of the bridge disorder on the average electronic coupling $\langle V_{DA} \rangle$ can be evaluated from (eqn (8)).

$$\langle V_{DA}(\omega, \varphi_1, \varphi_2, \dots, \varphi_{n-1}) \rangle_x = V_x \cdot \langle V(\omega) \rangle \cdot \prod_{m=1}^{x-1} \langle V(\varphi_m) \rangle = V_x \cdot \langle V(\omega) \rangle \cdot \langle V(\varphi) \rangle^{x-1} \qquad (8)$$

where V_x is the electronic coupling for a planar bridge and is here considered to be a bridge-length dependent constant. $\langle V(a) \rangle$ is an average given by:

$$\langle V(a) \rangle = \frac{\int V(a) e^{-E_{rot}(a)/RT} da}{\int e^{-E_{rot}(a)/RT} da} \qquad (9)$$

where a corresponds to any dihedral angle, ω or φ, and $E_{rot}(a)$ is the intrinsic energy barrier for rotating coordinate a. In this expression, the temperature-dependent conformational distribution is taken into account in the factors $\langle V(\omega) \rangle$ and $\langle V(\varphi) \rangle$ which also give the conformational dependence of the total electronic coupling. From the calculated $\langle V_{DA} \rangle$ values, the β-values at any temperature can be determined according to eqn (10).

$$\beta = -2 \frac{d \ln \langle V_{DA} \rangle}{d R_{DA}} \qquad (10)$$

where $\ln \langle V_{DA} \rangle$ can be re-written as a sum of three terms (eqn (11)).

$$\ln \langle V_{DA} \rangle = \ln V_x + \ln \langle V(\omega) \rangle + (x - 1) \ln \langle V(\varphi) \rangle \qquad (11)$$

From eqn (11), one can visualize which terms contribute to the temperature dependence and/or the bridge length dependence of the electronic coupling. The first term is temperature-independent (i.e. conformation-independent) but specific to the length of the bridge and the ensemble donor-bridge-acceptor used (i.e. ΔE_{DB}). The second and third terms depend on conformation and "carry" the temperature dependence of the electronic coupling. However, the former is independent of the bridge length, hence will not contribute to β. In contrast the last term vary with the size of the bridge, hence is the only term contributing to the temperature dependence of β. One can thus express the attenuation factor β_{tot} as the sum of two independent parts, one temperature-independent $\beta_0(\Delta E_{DB})$ and one temperature-dependent $\beta(T)$ that reflects the effect of the bridge conformational disorder at temperature T.

$$\beta_{tot} = \beta_0(\Delta E_{DB}) + \beta(T) \qquad (12)$$

This expression is believed to be quite general and prevails for any series of D-B-A systems consisting of several identical repeating bridge units. The temperature independent term $\beta_0(\Delta E_{DB})$ gives the lowest obtainable β-value for a given repeating bridge structure (e.g. for a planar OPE bridge). Fig. 10 compares the experimental and calculated β-values for the TEET rates in the series ZnP-nB-H$_2$P (n = 2-5) as a function of temperature. At high temperature (i.e. low solvent viscosity), the calculated β-values agree very well with the experimental values, supporting the validity of the model based on a Boltzmann description of the bridge conformational disorder. However, at low temperature, i.e. at high viscosity, the experimental β-values decrease much faster than predicted. In the high viscosity regime, corrections to the model are required in order to take into account the increased solvent viscosity that may hinder rotational motions. In other words, the potential energy associated to the conformational configuration $E_{rot}(a)$ in eqn (9) varies with the viscosity of the solvent. To correct for this, $E_{rot}(a)$ was

replaced by a temperature-dependent apparent activation barrier. This allowed to successfully modeling the experimental temperature dependence of the attenuation factor over the entire temperature range 80 K - 200 K (see solid line in Fig. 10).
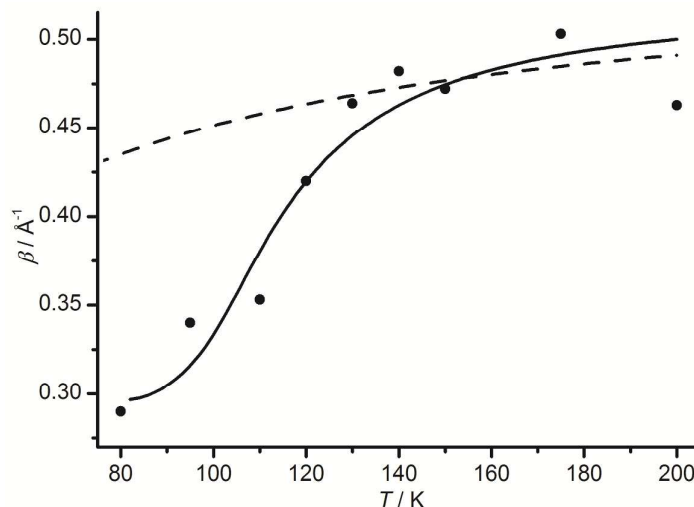
Fig. 10 Comparison between experimentally determined β-values versus temperature ($\bullet$) and fits of the theoretical model using a pure Boltzmann averaging (dashed line) and using viscosity-dependent activation energy (solid line). Reprinted from "Temperature Dependence of Electronic Coupling through Oligophenyleneethynylene Bridges" Mattias P. Eng, Jerker Mårtensson, Bo Albinsson. Chemistry - A European Journal, 14, 2819. Copyright © 2008 WILEY-VCH Verlag GmbH & Co. KGaA, Weinheim. Reproduced with permission.

More generally it was demonstrated that for D-B-A systems in which internal rotational dynamics are much faster than the transfer rates, conformational dependence of the electronic coupling and the β-value can be well described by considering a pure Boltzmann distribution of conformations. However when rotational dynamics and transfer rates occur on the same timescale (i.e. at low temperature and/or high viscosity), a pure Boltzmann conformational distribution is not accurate anymore as it tends to favor the population of conformations with the minimum rotational energy barrier (i.e. intrinsic energy). Finally, it was established that for all bridge structures with potential energy minima associated with a planar conformation ($\varphi = 0°$), the maximum conformational effect on the β-value is simply given by the number $2ln2/R_0$ where R_0 is the length of a single bridge unit. This leads to the conclusion that although $\beta_0(\Delta E_{DB})$ is system specific, $\beta(T)$ is a bridge specific parameter which is independent of the donor/acceptor couple used and whose maximum value can be predicted.

5. Porphyrin-based molecular wires

Porphyrins are planar 18π-electron conjugated macrocycles built from four pyrrole units and four methine carbons. One particularity of these structures is the strong sensitivity of their conjugated electronic system on substitution at the peripheric positions, namely α, β and *meso* (Fig. 11A). In multiporphyrin arrays, perturbations of the conjugated electronic system of individual porphyrins often lead to unusual electronic and optical properties. In the last decade, multiporphyrin arrays, due to their unusual electronic behavior, have attracted much interest, in view of potential applications in molecular electronics, photovoltaics and non-linear optics.[9] A wide range of multiporphyrin arrays have been synthesized with architectures going from simple linear structures to cyclic, box, and grid-like structures. To realize such constructs, the porphyrins are connected either directly to each other or using a linker. Different linkers have been used including phenyls[33], alkenes[34] or alkynes[34b, 34c, 35]. It is now widely accepted that the type of linker and the porphyrin linkage topology (α, β or *meso*) govern the inter-porphyrin electronic coupling in these arrays, hence their photophysical properties. In the following section, we restrict the discussion to only linear multiporphyrin arrays and emphasize a few examples that focus on the relationship between the electronic structure and the photophysical properties. Also synthetic methodologies to obtain these multiporphyrin arrays fall out of the scope of this tutorial review. Recent advances in synthesis of multiporphyrin arrays have been nicely reviewed by Osuka and co-workers.[36]

Systems containing one, two or more porphyrin units were primarily designed as mimics of the light harvesting antenna complexes in natural photosynthesis. Donor or acceptors were attached to the porphyrins to form donor-acceptor systems and the porphyrins played the role of primary electron donors. In these systems, excitation of the porphyrins lead first to the formation of a charge separated state, thereafter a cascade of electron-transfer events takes place separating the charges both spatially and temporally.[33a, 37] In this context, most studies have focused on producing extremely long-lived charge-separated states that might allow for subsequent chemical reactions to occur. The groups of Gust,[33a] Osuka[33c] and Fukuzumi[37] reported promising porphyrin-based systems showing long-lived charge-separated states following photo-excitation. In all these examples, the porphyrins connected using phenyl linkers at their *meso* positions are not strongly conjugated (i.e. electronically coupled). Due to steric hindrance with the β-substituents, the phenyl linkers are forced to adopt a nearly orthogonal arrangement with the porphyrin plane. This orthogonal arrangement breaks the conjugation and leads to a weak electronic coupling between the individual porphyrins. This configuration has been used by Lindsey and co-workers to design a molecular photonic wire for efficient singlet energy transfer.[38] They used *meso-meso* diphenylethyne-linked porphyrin oligomers, in which conjugation (i.e. electronic coupling) was intentionally minimized to avoid competition between energy transfer and electron transfer quenching. For steric reasons, directly linked *meso-meso* porphyrins show also weak inter-porphyrin electronic coupling.[8c] To transport charge over long distances, the porphyrin units need to be connected in a different way and construct a "supermolecule" with strong electronic communication. Several strategies have been reported to construct large networks of conjugated

porphyrins, that differ essentially by the type of linker used and the porphyrin linkage topology (β-β, *meso-meso*, *meso*-β). The groups of Therien[35], Anderson[34b, 34c] and Smith[34a] have used unsaturated linkers such as alkynes and alkenes (Fig. 11B & 11C). Other groups, i.e. Osuka et al.[39] and Crossley et al.[40], have synthesized fused porphyrin arrays, in which the porphyrin monomers are directly connected using multiple covalent bonds (Fig. 11D) or an aromatic linker.
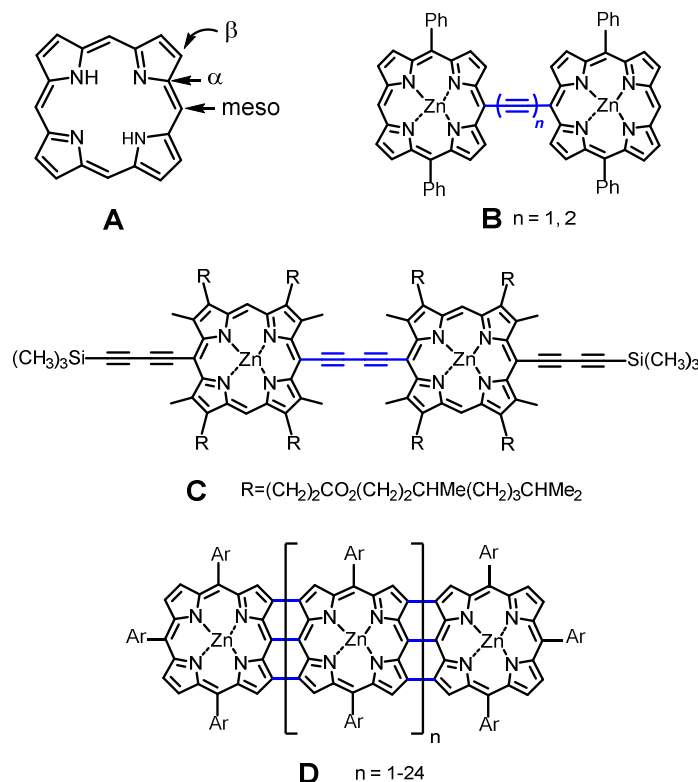
Fig. 11 (A) Molecular structure of a free-base porphyrin indicating the different peripheric positions for substitution: α, β and *meso*. **(B-D)** Molecular structures of different strongly conjugated porphyrin oligomers synthetized by the groups of **(B)** Therien[35], **(C)** Anderson[34b] and **(D)** Osuka[39b].

5.1 Strongly coupled porphyrin oligomers

Bridging porphyrins using alkyne linkers is not a new idea; already in 1978, Arnold and co-workers reported a nickel porphyrin dimer bridged at its *meso* position by 1,3-butadiyne linker.[41] The strong inter-porphyrin electronic coupling in this dimer was evidenced by strong alteration of its ground-state absorption spectrum compared to the monomer. Since this first report, alkyne-linked porphyrin oligomers have been intensively investigated, in particular with respect to structure-property relationships. In 1990s, the groups of Therien[35] and Anderson[34b] synthesized zinc porphyrin dimers connected at their *meso* position using ethyne and butadiyne linkers, respectively (Fig. 11B & 11C). In both cases, in contrast to phenyl linkers, alkynes allow a coplanar arrangement of the porphyrin planes resulting in a significant π-overlap between the porphyrin macrocyles. This ensures a strong inter-porphyrin electronic coupling in the ground-state. In the excited state, one observes an even stronger

electronic coupling due, to on average, a more planar conformation of the oligomers than in the ground-state.[42] This results from the enhanced charge delocalization in the excited states.[8b] Therien and co-workers investigated further the effect of the porphyrin linkage topology on the electronic coupling by preparing two series of *meso-meso*, *meso-β* and *β-β* linked porphyrin dimers, related to the ones in Fig. 11B.[8a] They employed ethyne linkers in one series and butadiyne linkers in the other series. For both series, the *meso-meso* connectivity resulted in maximum inter-porphyrin electronic coupling. The *meso-β* and *β-β* connectivity had weaker electronic communication between the porphyrins. For the ethyne-linked dimers, this could be explained by sterical constraints, forcing the linker to twist out of the porphyrin plane. In the butadiyne-linked series, the reduced conjugation in *meso-β* and *β-β* linked dimers was ascribed to smaller orbital overlap at the β position. In a similar context, Anderson and co-workers have thoroughly investigated the effect of enhanced conjugation on the photophysical properties of a series of 1,3-butadiyne linked zinc porphyrin oligomers denoted P_n, spanning from monomer P_1 to octamer P_8.[34c] Fig. 12 shows the absorption spectra of the entire series P_n (n = 1-4, 6, 8). The ground-state absorption spectra of P_n (n $\geq$ 2) are markedly altered by the extensive conjugation and clearly do not resemble the spectrum of the monomer P_1. In particular the lowest absorption band (the Q-band) gradually red-shifts with the size of the oligomer and gets significantly stronger. The gradual red-shift of the Q band with the length of the oligomer was also nicely reproduced by TD-DFT (B3LYP/6-31G*) calculations of the lowest electronic transitions in the Q band spectral region (Fig. 12).[43] For simplicity, these calculations were performed assuming coplanar porphyrins for the entire series P_n (n = 1-4, 6, 8). Also earlier computational calculations of the electronic spectra of the dimer by Beljonne et al.[44] demonstrated the enhanced stabilization of the excited states. The calculated and experimental absorption spectra closely agreed only when considering a reduction of the bond length alternation in the central butadiyne in the excited state geometry of the dimer, hence indicating an increased conjugation in the excited state. Another manifestation of the enhanced conjugation is the reduction of the HOMO-LUMO gap which is related to the experimental E_{00} energy of the lowest electronic transition. Experimentally E_{00} might be evaluated from the wavelength corresponding to the intersection of the normalized absorption and emission spectra. For the conjugated porphyrin oligomers P_n (n= 1-4, 6, 8), E_{00} decreases gradually from about 1.9 eV for P_1 to less than 1.5 eV for P_8. This reduction of E_{00} has been attributed mainly to stabilization of the LUMO orbitals (i.e. the excited states).[8b] Another advantage that should be highlighted, is the relatively large size of the monomer unit in these conjugated porphyrin oligomers which allows a distance coverage of approximately 12 nm for the longest member of the series, P_8. This, in addition to their attractive electronic properties, makes them excellent candidates for charge/energy transport over long distances.
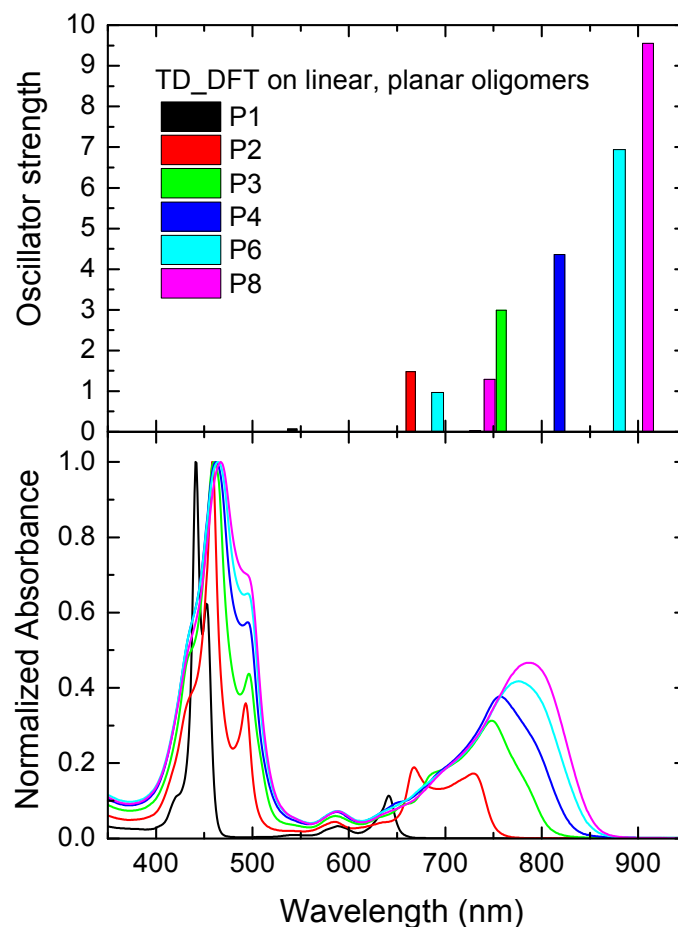
Fig. 12 (top) Calculated (TDDFT: B3LYP/6-31G*) ground-state stick spectra for the planar conformer of P_1 (black), P_2 (red), P_3 (green), P_4 (blue), P_6 (cyan) and P_8 (magenta) in the Q-band region. **(bottom)** Normalized ground-state absorption spectra of P_1 (black), P_2 (red), P_3 (green), P_4 (blue), P_6 (orange) and P_8 (magenta). Note: the electronic absorption spectrum of a typical zinc porphyrin P_1 serves as a reference and consists of a strong transition band to the second excited state at about 400 nm, generally called the Soret band, and a weaker transition band to the first excited state at about 550 nm, called the Q band.

Although alkyne linkers seem to be "ideal" linkers to achieve strong inter-porphyrin electronic coupling, alkyne-linked porphyrin oligomers possess a rod-like structure but are not strictly constrained planar systems. At room temperature, the alkyne linkers allow an almost barrierless rotation of individual porphyrin units. The individual porphyrin moieties can almost freely move in and out of the plane, reducing the inter-porphyrin electronic coupling. This results in a wide distribution of rotational conformers in the ground-state, as evidenced by the spectrally broad Q-band which for the longer oligomers increases in width as the number of conformational degrees of freedom increases (Fig. 12). Although conformational heterogeneity may seem to constitute a drawback for application of these conjugated porphyrin oligomers as molecular wires, inducing conformational

changes have been successfully used as a way to regulate the electron flow and charge separation in D-B-A systems bridged by conjugated porphyrin oligomers.[7b, 43, 45] To construct strictly coplanar and strongly coupled porphyrin oligomers, several approaches have been proposed. Fused porphyrin oligomers (also called porphyrin tapes) are realized by connecting the porphyrins either indirectly through an aromatic linker or directly by covalent bonds at their *meso* and β positions. In general, the strong inter-porphyrin electronic coupling in these porphyrin oligomers results in strongly red-shift absorption bands, that makes them interesting systems for non-linear optical applications. The aromatic-linker approach has been used by Crossley and co-workers who synthesized several β-β fused porphyrin oligomers via aromatic linkers.[40] More recently Anderson et al. also synthesized *meso*-β fused porphyrin dimers displaying red-shifted absorption bands at 1.15 eV.[46] Fused porphyrin oligomers triply linked at their meso, β, β positions by covalent bonds, reported by Osuka and co-workers, exhibit even stronger electronic coupling with strongly red-shifted Q-bands at only 0.43 eV for a 12-mer fused array (Fig. 11D).[39]

5.2 Electron transfer in porphyrin-based molecular wires

Owing to their strong inter-porphyrin electronic coupling, alkyne and alkene-linked porphyrin oligomers are expected to sustain efficient charge transport over long distances. This has been shown experimentally in several studies both at an ensemble and single molecule levels. At the ensemble level, spectroscopic techniques such as EPR and pump-probe transient absorption have been used. In particular analysis of EPR spectra provides information on the number of sites over which a radical cation is delocalized or hops. For instance, Therien and co-workers have used EPR spectroscopy to probe the mobility of the radical cation states in *meso-meso* ethyne-linked zinc porphyrin oligomers related to the ones presented in Fig. 11B.[47] They reported a hole-delocalization length of more than 50 Å for the radical cation state in the pentamer over the entire temperature domain 4 K – 298 K. Also hole motion in this oligomer was found to be temperature-independent, pointing towards a full delocalization of the hole in the ground-state rather than a hole motion by hopping. Later in a similar work, Wasielewski and co-workers demonstrated by EPR spectroscopy efficient charge mediation in singly oxidized *meso-meso* and meta-phenylene-linked zinc porphyrin dimers, as well as in a dodecameric ring consisting of six *meso-meso* linked porphyrin dimers covalently connected by a phenyl linker.[48] In these systems, charge motion was found to be temperature-dependent, indicating a hopping mechanism. At room temperature, rapid hole hopping with rates exceeding 10^7 s^{-1} was observed in the dimer and in the dodecameric ring spanning 8-12 porphyrins. However upon lowering the temperature to 180 K, hole motion slowed down for all systems and the EPR line of all radical cations resembled the one of the reference monomer, pointing towards a trapping of the radical cation on a single porphyrin unit. Nevertheless, this example illustrates that despite a weaker inter-porphyrin electronic coupling (discussed earlier), *meso-meso* linked porphyrin oligomers are capable of mediating charge efficiently. Remarkably, the hole can hop rapidly among 8-12 porphyrins in the

cyclic array, a distance that is nearly the same as the one observed among BChls in the natural light harvesting systems LH1.[49]

Femtosecond pump-probe transient absorption was used by Winters et al. to investigate electron transfer in butadyine-linked porphyrin oligomers.[50] Charge recombination was studied in a homologeous series of D-B-A systems $Fc^+-P_n-C_{60}^-$ (n = 1, 2, 4), in which butadiyne-linked porphyrin oligomers of different lengths were used to bridge the electron donor (C_{60}^-) and the electron acceptor (Fc^+). In these D-B-A systems, the fully charge-separated state $Fc^+-P_n-C_{60}^-$ was formed after photo-excitation of the porphyrin oligomer and a subsequent series of charge transfer steps. Recombination of this fully charge-separated state $Fc^+-P_n-C_{60}^-$ was followed by transient absorption. It was shown that the charges recombine very efficiently, even for the longer bridge P_4 corresponding to a donor-acceptor separation of 65 Å. More interestingly, similar recombination rates for n = 2 and n = 4 were observed, giving a very small apparent attenuation factor, $\beta = 0.003$ Å^{-1}. The non-exponential and weak distance dependence of the recombination rates suggested an incoherent hopping process. However no clear evidence of hopping was observed and it was concluded that recombination was more likely to occur via coherent electron tunneling. The fact that the distance dependence in this case fell out of the McConnell model was ascribed to assumptions in the model. As mentioned in the theoretical part, one requirement of the McConnell model is a weak coupling between the bridge sub-units, V_{BB} compared to the tunneling energy barrier ΔE. In butadiyne-linked porphyrin oligomers, the inter-porphyrin electronic coupling is quite strong due to the significant π-overlap between the porphyrin macrocles. The similar recombination rates for $Fc^+-P_2-C_{60}^-$ and $Fc^+-P_4-C_{60}^-$ suggest that butadiyne-linked porphyrin oligomers can be regarded as continuous tunneling barriers. Thus in these D-B-A systems, conditions of the McConnell model might not be fulfilled. This implies that the McConnell model is not appropriate to describe the electron-transfer distance dependence in the $Fc^+-P_n-C_{60}^-$ systems, or more generally, in any strongly conjugated system.

Recently, although outside the scope of this tutorial review, single molecule experiments that allow probing the conductivity of porphyrin molecular wires have been reported by the groups of Anderson and Therien.[3a, 3c] This is realized by placing a porphyrin oligomer between two metallic contacts in an STM break-junction configuration and measuring its molecular conductance. This molecular conductance can be compared to the electronic coupling V_{DA} in D-B-A systems obtained through photophysical measurements. It generally decreases exponentially upon lengthening of the oligomer with a slope β related to the attenuation factor for electron transfer. Sedgi et al. measured the conductance of a series of butadiyne-linked porphyrin oligomers similar to the ones described previously and demonstrated their wire-like behavior with a low attenuation factor, $\beta = 0.04$ Å^{-1}.[3a] Their results agreed with the apparent low attenuation factor reported for photo-induced charge transfer in $Fc-P_n-C_{60}$ systems.[50] Nevertheless, one should note that only trends in the attenuation factor can be compared. The absolute β-values obtained in these two sets of experiments are not comparable

due to the different tunneling energy barriers. In an extended study, Sedgi et al. also compared the molecular conductance of three types of porphyrin oligomers with a pyridyl anchoring group: *meso-meso* butadiyne-linked oligomers, twisted *meso-meso* linked oligomers and *meso-meso*, β-β, β-β triply linked oligomers.[3b] As expected, the fused arrays have the lowest attenuation factor of 0.02 Å^{-1}, followed by *meso-meso* butadiyne-linked arrays with $\beta = 0.04$ Å^{-1} and finally twisted *meso-meso* linked arrays with $\beta = 0.11$ Å^{-1}. This can be rationalized by the stronger inter-porphyrin electronic coupling that results from the coplanar orientation of the porphyrin macrocycles in fused porphyrin arrays.

5.3 Excitation energy transfer in porphyrin-based molecular wires

In the following section, excitonic coupling in multiporphyrin arrays is discussed. In particular we would like to highlight the difference between exciton coupling and electron delocalization caused by stronger electronic coupling, and emphasize the fact that exciton coupling is a major effect in weakly conjugated porphyrin systems, while the effects of overlapping π-orbitals generally dominate the spectroscopy of strongly conjugated porphyrin systems. In a multichromophoric system, exciton coupling reflects the collective behavior of all individual transition dipole moments. In contrast, stronger electronic coupling can be understood as the extent of electronic delocalization that results from the π-orbital overlap. Directly *meso-meso* linked multiporphyrin arrays which are weakly conjugated systems have been thoroughly investigated by Osuka and co-workers.[8c] They explored the effect of exciton coupling on the photophysical properties of these systems. A first simple manifestation of exciton coupling in these systems is the spectral changes in the Soret bands of their absorption spectra. Upon lengthening of the oligomer (for n ≥ 2), the Soret band splits into two components whose relative intensity depends on the number of porphyrin units. The most red-shifted exciton coupling band corresponds to a coplanar head-to-tail configuration of the individual porphyrin transition moments. As the size of the oligomer increases, this red-shifted band gets stronger. Both the splitting of the Soret band and relative intensity of its components can be explained using the point dipole exciton coupling theory developed by Kasha.[18] However the Q-band remains almost unperturbed with the size of the oligomer. This differs from the case of *meso-meso* butadiyne-linked and fused porphyrin oligomers discussed earlier, where the Q-band gradually red-shifts and gets stronger with the size of the oligomer. In these systems, strong electronic coupling effects dominate over exciton coupling effects due to the larger π-orbital overlap between the "close to coplanar" porphyrin macrocycles. In directly *meso-meso* linked porphyrin oligomers, electron delocalization is hindered by the perpendicular orientation of the porphyrin moieties, hence the modest spectral changes observed in the Q-band with increasing length of the oligomer.

6. Conclusion

Over the last decades, photoinduced charge and energy transfer in donor-bridge-acceptor (D-B-A) systems has been thoroughly investigated, as demonstrated by the vast literature in this field. This tutorial review presents a few representative examples to illustrate the role played by the molecular bridge. It has been shown both theoretically and experimentally that the bridge is not a simple spectator, and that its energetics and conformational dynamics strongly influence the charge/energy transport (kinetics). Numerous studies of the distance dependence of transfer rates have shown that the current knowledge is not sufficient to *a priori* predict the charge transport mechanism or when charge transport will occur over long distances. Interpretation of these studies was often hampered by simultaneous variation of the width and height of the tunneling energy barrier. However, careful design of the D-B-A systems could allow access to distance, energy gap (section 3.1 and 3.2) and conformational effects (section 4.1) on the donor-acceptor electronic coupling, hence the kinetics of the transfer rates. Achieving a wire-like behavior of the bridge, i.e. small distance dependence of the charge transport, has been demonstrated for fluorene and phenylvinylene-bridged D-B-A systems in which charge transport occurs in the hopping regime. However, other D-B-A system based on fluorenone bridge units, in which charge transport also occurs via incoherent hopping, showed a stronger distance dependence of the transfer rate constants. All these studies illustrate that there is still a need to establish methods for predicting when wire-like properties and weak distance dependence is expected. Other promising systems for charge and/or energy transport are multiporphyrin-arrays, whose photophysical properties can be tuned by modifying the type of linker and the porphyrin linkage topology. Finally, the next step ahead is transfer of the knowledge learnt from studies of photoinduced charge/energy transport in D-B-A systems to the development of molecular-based devices and thereby contributing to the solution of huge societal challenges such as the demand for clean energy.

Acknowledgements

References

1 G. D. Scholes, G. R. Fleming, A. Olaya-Castro and R. van Grondelle, *Nat Chem*, 2011, **3**, 763.
2 (a) D. Gust, T. A. Moore and A. L. Moore, *Faraday Discuss.*, 2012, **155**, 9; (b) M. R. Wasielewski, *Acc. Chem. Res.*, 2009, **42**, 1910.
3 (a) G. Sedghi, K. Sawada, L. J. Esdaile, M. Hoffmann, H. L. Anderson, D. Bethell, W. Haiss, S. J. Higgins and R. J. Nichols, *J. Am. Chem. Soc.*, 2008, **130**, 8582; (b) G. Sedghi, L. J. Esdaile, H. L. Anderson, S. Martin, D. Bethell, S. J. Higgins and R. J. Nichols, *Adv. Mater.*, 2012, **24**, 653; (c) Z. Li, T.-H. Park, J. Rawson, M. J. Therien and E. Borguet, *Nano Lett.*, 2012, **12**, 2722.
4 H. McConnell, *Journal of Chemical Physics*, 1961, **35**, 508.

5 (a) B. Albinsson and J. Mårtensson, *Journal of Photochemistry and Photobiology C: Photochemistry Reviews*, 2008, **9**, 138; (b) O. S. Wenger, *Chem. Soc. Rev.*, 2011, **40**, 3538.

6 (a) W. B. Davis, W. A. Svec, M. A. Ratner and M. R. Wasielewski, *Nature*, 1998, **396**, 60; (b) W. B. Davis, M. A. Ratner and M. R. Wasielewski, *Chem. Phys.*, 2002, **281**, 333; (c) K. Pettersson, J. Wiberg, T. Ljungdahl, J. Mårtensson and B. Albinsson, *J. Phys. Chem. A*, 2005, **110**, 319; (d) D. Hanss and O. S. Wenger, *Inorg. Chem.*, 2008, **48**, 671.

7 (a) A. C. Benniston and A. Harriman, *Chem. Soc. Rev.*, 2006, **35**, 169; (b) M. U. Winters, J. Kärnbratt, H. E. Blades, C. J. Wilson, M. J. Frampton, H. L. Anderson and B. Albinsson, *Chem. Eur. J.*, 2007, **13**, 7385; (c) D. Hanss, M. E. Walther and O. S. Wenger, *Coord. Chem. Rev.*, 2010, **254**, 2584; (d) C. Schubert, M. Wielopolski, L.-H. Mewes, G. de Miguel Rojas, C. van der Pol, K. C. Moss, M. R. Bryce, J. E. Moser, T. Clark and D. M. Guldi, *Chem. Eur. J.*, 2013, **19**, 7575.

8 (a) V. S. Y. Lin and M. J. Therien, *Chem. Eur. J.*, 1995, **1**, 645; (b) H. L. Anderson, *Chem. Commun.*, 1999, 2323; (c) D. Kim and A. Osuka, *Acc. Chem. Res.*, 2004, **37**, 735.

9 D. Kim, *Multiporphyrin Arrays: Fundamentals and Applications*, Pan Stanford, 2012.

10 F. Giacalone, J. L. Segura, N. Martín and D. M. Guldi, *J. Am. Chem. Soc.*, 2004, **126**, 5340.

11 G. de la Torre, F. Giacalone, J. L. Segura, N. Martin and D. M. Guldi, *Chem.-Eur. J.*, 2005, **11**, 1267.

12 (a) K. Kilså, J. Kajanus, A. N. Macpherson, J. Mårtensson and B. Albinsson, *J. Am. Chem. Soc.*, 2001, **123**, 3069; (b) J. Wiberg, L. Guo, K. Pettersson, D. Nilsson, T. Ljungdahl, J. Mårtensson and B. Albinsson, *J. Am. Chem. Soc.*, 2006, **129**, 155.

13 C. Atienza, N. Martin, M. Wielopolski, N. Haworth, T. Clark and D. M. Guldi, *Chem. Commun.*, 2006, 3202.

14 (a) E. A. Weiss, M. J. Ahrens, L. E. Sinks, A. V. Gusev, M. A. Ratner and M. R. Wasielewski, *J. Am. Chem. Soc.*, 2004, **126**, 5577; (b) E. A. Weiss, M. J. Tauber, R. F. Kelley, M. J. Ahrens, M. A. Ratner and M. R. Wasielewski, *J. Am. Chem. Soc.*, 2005, **127**, 11842.

15 (a) R. H. Goldsmith, L. E. Sinks, R. F. Kelley, L. J. Betzen, W. H. Liu, E. A. Weiss, M. A. Ratner and M. R. Wasielewski, *Proc. Natl. Acad. Sci. U. S. A.*, 2005, **102**, 3540; (b) T. Miura, R. Carmieli and M. R. Wasielewski, *J. Phys. Chem. A*, 2010, **114**, 5769.

16 C. Atienza-Castellanos, M. Wielopolski, D. M. Guldi, C. van der Pol, M. R. Bryce, S. Filippone and N. Martin, *Chem. Commun.*, 2007, 5164.

17 A. B. Ricks, K. E. Brown, M. Wenninger, S. D. Karlen, Y. A. Berlin, D. T. Co and M. R. Wasielewski, *J. Am. Chem. Soc.*, 2012, **134**, 4581.

18 M. Kasha, H. Rawls and M. A. El-Bayoumi, *Pure Appl. Chem*, 1965, **11**, 371.

19 (a) R. A. Marcus, *J. Chem. Phys.*, 1965, **43**, 679; (b) R. A. Marcus, *J. Chem. Phys.*, 1956, **24**, 966.

20 (a) J. Jortner and M. Bixon, *J. Chem. Phys.*, 1988, **88**, 167; (b) J. Ulstrup and J. Jortner, *J. Chem. Phys.*, 1975, **63**, 4358.

21 (a) Y. A. Berlin, G. R. Hutchison, P. Rempala, M. A. Ratner and J. Michl, *J. Phys. Chem. A*, 2003, **107**, 3970; (b) Y. A. Berlin, A. L. Burin and M. A. Ratner, *Chem. Phys.*, 2002, **275**, 61.

22 (a) M. U. Winters, K. Pettersson, J. Mårtensson and B. Albinsson, *Chem. Eur. J.*, 2005, **11**, 562; (b) B. P. Paulson, J. R. Miller, W. X. Gan and G. Closs, *J. Am. Chem. Soc.*, 2005, **127**, 4860; (c) E. A. Weiss, M. R. Wasielewski and M. A. Ratner, in *Molecular Wires: From Design to Properties*, ed. L. DeCola, Springer-Verlag Berlin, Berlin, 2005, vol. 257, pp. 103.

23 K. Kilså, J. Kajanus, J. Mårtensson and B. Albinsson, *J. Phys. Chem. B*, 1999, **103**, 7329.

24 W. B. Davis, M. A. Ratner and M. R. Wasielewski, *J. Am. Chem. Soc.*, 2001, **123**, 7877.

25 M. E. Walther, J. Grilj, D. Hanss, E. Vauthey and O. S. Wenger, *Eur. J. Inorg. Chem.*, 2010, **2010**, 4843.

26 D. Hanss and O. S. Wenger, *Inorg. Chem.*, 2008, **47**, 9081.

27 M. P. Eng and B. Albinsson, *Chem. Phys.*, 2009, **357**, 132.

28 D. Hanss and O. S. Wenger, *Eur. J. Inorg. Chem.*, 2009, **2009**, 3778.

29 G. L. Closs, M. D. Johnson, J. R. Miller and P. Piotrowiak, *J. Am. Chem. Soc.*, 1989, **111**, 3751.

30 A. C. Benniston, A. Harriman, P. Li, P. V. Patel and C. A. Sams, *Phys. Chem. Chem. Phys.*, 2005, **7**, 3677.

31 M. P. Eng, J. Mårtensson and B. Albinsson, *Chem. Eur. J.*, 2008, **14**, 2819.

32 (a) M. P. Eng and B. Albinsson, *Angew. Chem.*, 2006, **118**, 5754; (b) M. P. Eng, T. Ljungdahl, J. Mårtensson and B. Albinsson, *J. Phys. Chem. B*, 2006, **110**, 6483.

33 (a) R. E. Palacios, G. Kodis, S. L. Gould, L. de la Garza, A. Brune, D. Gust, T. A. Moore and A. L. Moore, *ChemPhysChem*, 2005, **6**, 2359; (b) A. Osuka, S. Nakajima, K. Maruyama, N. Mataga, T. Asahi, I. Yamazaki, Y. Nishimura, T. Ohno and K. Nozaki, *J. Am. Chem. Soc.*, 1993, **115**, 4577; (c) A. Osuka, N. Mataga and T. Okada, *Pure & Appl. Chem.*, 1997, **69**, 797.

34 (a) M. O. Senge, K. R. Gerzevske, M. G. H. Vicente, T. P. Forsyth and K. M. Smith, *Angew. Chem. Int. Ed. Engl.*, 1993, **32**, 750; (b) H. L. Anderson, S. J. Martin and D. D. C. Bradley, *Angew. Chem. Int. Ed. Engl.*, 1994, **33**, 655; (c) P. N. Taylor, J. Huuskonen, R. T. Aplin, H. L. Anderson, G. Rumbles and E. Williams, *Chem. Commun.*, 1998, 909.

35 V. Lin, S. DiMagno and M. Therien, *Science*, 1994, **264**, 1105.

36 (a) T. Tanaka and A. Osuka, *Chem. Soc. Rev.*, 2014; (b) Y. Nakamura, N. Aratani and A. Osuka, *Chem. Soc. Rev.*, 2007, **36**, 831.

37 H. Imahori, Y. Sekiguchi, Y. Kashiwagi, T. Sato, Y. Araki, O. Ito, H. Yamada and S. Fukuzumi, *Chem. Eur. J.*, 2004, **10**, 3184.

38 R. W. Wagner and J. S. Lindsey, *J. Am. Chem. Soc.*, 1994, **116**, 9759.

39 (a) A. Tsuda and A. Osuka, *Science*, 2001, **293**, 79; (b) T. Ikeda, N. Aratani and A. Osuka, *Chem. Asian J.*, 2009, **4**, 1248.

40 T. Khoury and M. J. Crossley, *Chem. Commun.*, 2007, 4851.

41 D. P. Arnold, A. W. Johnson and M. Mahendran, *J. Chem. Soc., Perkin Trans. 1*, 1978, 366.

42 M. U. Winters, J. Kärnbratt, M. Eng, C. J. Wilson, H. L. Anderson and B. Albinsson, *J. Phys. Chem. C*, 2007, **111**, 7192.

43 M. Gilbert, L. J. Esdaile, M. Hutin, K. Sawada, H. L. Anderson and B. Albinsson, *J. Phys. Chem. C*, 2013, **117**, 26482.

44 D. Beljonne, G. E. O'Keefe, P. J. Hamer, R. H. Friend, H. L. Anderson and J. L. Brédas, *J. Chem. Phys.*, 1997, **106**, 9439.

45 J. Kärnbratt, M. Hammarson, S. Li, H. L. Anderson, B. Albinsson and J. Andréasson, *Angew. Chem. Int. Ed.*, 2010, **49**, 1854.

46 M. Pawlicki, M. Morisue, N. K. S. Davis, D. G. McLean, J. E. Haley, E. Beuerman, M. Drobizhev, A. Rebane, A. L. Thompson, S. I. Pascu, G. Accorsi, N. Armaroli and H. L. Anderson, *Chem. Sci.*, 2012, **3**, 1541.

47 K. Susumu, P. R. Frail, P. J. Angiolillo and M. J. Therien, *J. Am. Chem. Soc.*, 2006, **128**, 8380.

48 T. M. Wilson, T. Hori, M.-C. Yoon, N. Aratani, A. Osuka, D. Kim and M. R. Wasielewski, *J. Am. Chem. Soc.*, 2010, **132**, 1383.

49 D. Kolbasov, N. Srivatsan, N. Ponomarenko, M. Jäger and J. R. Norris, *J. Phys. Chem. B*, 2003, **107**, 2386.

50 M. U. Winters, E. Dahlstedt, H. E. Blades, C. J. Wilson, M. J. Frampton, H. L. Anderson and B. Albinsson, *J. Am. Chem. Soc.*, 2007, **129**, 4291.

TOC Figure

This tutorial review focuses on photo-induced charge/energy transfer in covalently linked donor-bridge-acceptor (D-B-A) systems.